Journal of *Marine Science and Engineering*

MDPI

Article

Operational Strategies for *CII* Under Short Voyages: Hybrid Denominator Correction and CPP Mode Optimization

Ji-Woong Lee, Quang Dao Vuong and Jae-Ung Lee *

Division of Marine System Engineering, National Korea Maritime and Ocean University, Busan 49112, Republic of Korea; woongsengine@kmou.ac.kr (J.-W.L.); quangdao.mtb@gmail.com (Q.D.V.)
* Correspondence: julee@kmou.ac.kr; Tel.: +82-(0)51-410-4662

Abstract

This study addresses structural distortions in the IMO Carbon Intensity Indicator (*CII*) for short-voyage training vessels and proposes corrective strategies combining denominator adjustments with controllable pitch propeller (CPP) mode optimization. Using 2024 operational data from a training ship, we computed monthly and annual *CII* values, identifying significant inflation when time-at-sea fractions are low due to extensive port stays. Two correction methods were evaluated: a hybrid denominator approach converting port-stay CO_2 to equivalent distance, and a Braidotti functional correction. The CPP operating maps for combination and fixed modes revealed a crossover point at approximately 12 kn (~50% engine load), where the combination mode shows superior efficiency at low speeds and the fixed mode at higher speeds. The hybrid correction effectively stabilized *CII* values across varying operational conditions, while the speed-band CPP optimization provided additional reductions. Results demonstrate that combining optimized CPP mode selection with hybrid *CII* correction achieves compliance with required standards, attaining a B rating. The integrated framework offers practical solutions for *CII* management in short-voyage operations, addressing regulatory fairness while improving operational efficiency for training vessels and similar ship types.

Keywords: Carbon Intensity Indicator; controllable pitch propeller; ship decarbonization; maritime emissions; IMO regulations; operational optimization; training vessels; fuel efficiency; CPP mode selection; *CII* correction

check for updates

Academic Editor: Claudio Ferrari

Received: 8 September 2025
Revised: 9 October 2025
Accepted: 17 October 2025
Published: 20 October 2025

Citation: Lee, J.-W.; Vuong, Q.D.; Lee, J.-U. Operational Strategies for *CII* Under Short Voyages: Hybrid Denominator Correction and CPP Mode Optimization. *J. Mar. Sci. Eng.* **2025**, *13*, 2010. https://doi.org/10.3390/jmse13102010

Copyright: © 2025 by the authors. Licensee MDPI, Basel, Switzerland. This article is an open access article distributed under the terms and conditions of the Creative Commons Attribution (CC BY) license (https://creativecommons.org/licenses/by/4.0/).

1. Introduction

The International Maritime Organization (IMO) has been steadily tightening decarbonization rules for the shipping sector. Since 2023, the Energy Efficiency Existing Ship Index (EEXI) and the Carbon Intensity Indicator (*CII*) have quantified ships' energy efficiency and carbon performance and assigned annual ratings (A–E), thereby requiring both technical and operational improvements in ship management. In subsequent MEPC discussions, mid- and long-term measures have been fleshed out, including fuel GHG-intensity management, expanded real-time monitoring and reporting, and assessment on a Well-to-Wake basis. In this environment, operators must go beyond generic fuel-saving measures and pursue data-driven operational optimization alongside compliance strategies [1].

Within this context, the efficient characteristics of controllable pitch propeller (CPP) operating modes are of particular significance. Prior studies have largely described the differences in fuel use and performance between combinator (combination) and fixed (or constant) modes, but few have quantitatively linked those differences to *CII* compliance

under the interaction of monthly operating data and the regulatory formula. The training vessel considered in this study features short sailing distances and a high share of port stays, which create a structural disadvantage in *CII* (annual CO_2 divided by transport work). The denominator shrinks while the relative influence of auxiliaries (generators/boilers) remains large, artificially inflating *CII* regardless of propulsion efficiency. This can lead to regulatory penalties that are operational rather than technical in nature, calling for corrections to the metric together with a redesign of operating strategies.

The IMO's baseline transport-work definition for most ships is cgDIST, as the product of gross tonnage (GT) and distance. For cruise ships, an alternative cbDIST is defined using available lower berths (ALB) $\times$ distance [2]. For the training vessel (GT $\approx$ 9196; ALB $\leq$ 250), replacing GT with ALB would shrink the denominator by an order of magnitude and thus inflate the computed *CII*. Moreover, the hotel or leisure loads on a training ship are much smaller than on cruise ships, so cbDIST is not representative for this use-case. Accordingly, in this paper, we retain cgDIST as the baseline transport-work definition while adopting cruise-segment coefficients or required lines only for comparability of ratings in the absence of training vessel-specific factors.

The motivation for this study arises from the structural bias of the current *CII* when applied to short-voyage training vessels. Because these ships operate on short routes with frequent port stays, the denominator of the formula defined as transport work (GT $\times$ distance) becomes disproportionately small, while the auxiliary fuel use for generators and boilers remains significant. As a result, the attained *CII* is inflated even when propulsion efficiency is high, leading to unfairly high carbon intensity ratings that do not reflect the vessel's true operational performance. This distortion motivated the development of corrective approaches that combine a hybrid denominator formulation, which separates sailing and port-stay emissions, with the CPP mode optimization to represent actual operational efficiency more accurately.

This study addresses three questions as the following: (i) How do speed–load relationships differ by the CPP mode, and where does the crossover point (in speed and load) appear in real data? (ii) How can the *CII* distortions arising from short, intermittent voyages be mitigated—via a hybrid denominator (equivalent-distance) correction or a Braidotti functional correction [3]—and what are the limits of each? (iii) Based on these findings, to what extent can a speed-band mode-selection strategy improve annual *CII* relative to the required line?

We take a training vessel as a case study and use 2024 ABLOG monthly records (e.g., fuel, time, distance). The vessel is not directly subject to MARPOL *CII* and carries no cargo (up to 250 trainees); therefore, for official *CII* calculation, we adopt cruise-segment coefficients or formulae. In our data-driven modeling, we (1) estimate mode-specific speed–load maps via regression; (2) set SFOC (load) from engine specifications or reference curves and compute speed-wise fuel and CO_2 (ton/nm); and (3) define a hybrid *CII* by converting port-stay CO_2 into an equivalent distance that is added to the denominator. For comparison, we also apply the Braidotti correction to diagnose distortions in the monthly distribution of *ts* (time-at-sea fraction) versus *CII*.

The main findings are as follows: First, in monthly assessments, the official *CII* surges as *ts* decreases and produces outliers in months with little or no sailing. The hybrid correction stabilizes values even at low *ts*, while Braidotti is effective on average but exhibits over-correction when *ts* is very small. Second, regression on observed data reveals a crossover near 12 kn ($\approx$50% load), yielding the operational rule that the combinator mode should be used at low speeds, whereas the fixed mode is preferable at medium and high speeds. Applying speed-band switching yields a modest additional improvement

over all-fixed operation. Third, the optimized mode combined with the hybrid correction (Opt-hybrid) remains below the required line and achieves a B rating.

This study quantitatively links the CPP mode operation to the *CII* compliance for short-voyage training vessels. It identifies the speed–load crossover between combination and fixed modes, proposes a hybrid denominator correction for port-intensive operations, and demonstrates their combined effect in improving *CII* stability and fairness.

2. Literature Review

2.1. Escalation of IMO Decarbonization Rules and the EEXI/CII Regime

The IMO's Initial Strategy on the reduction of GHG emissions from ships (adopted in 2018) laid the foundation for a comprehensive regulatory framework. From 1 January 2023, the EEXI (a one-off, design-based index for existing ships $\geq$ 400 GT) and the *CII* (an annual, operational carbon-intensity rating for ships $\geq$ 5000 GT) entered into force, operationalizing short-term measures toward the 2030 ambition of at least a 40% reduction in carbon intensity versus 2008. The Strategy was revised in 2023 to strengthen ambition and set the workplan toward mid-term measures [4].

EEXI is a design-phase compliance check (one-time approval during a ship's life), whereas *CII* is an annual operational metric assigning A–E ratings [5].

At MEPC 83 (April 2025), IMO approved a package of mid-term measures, combining a fuel GHG-intensity standard and a global pricing mechanism. A formal adoption was scheduled for an extraordinary session in Autumn 2025, with entry into force in 2027. In parallel, MEPC 83 completed Phase 1 of the review of short-term measures and set *CII* reduction (Z) factors for 2027–2030 at 13.625%, 16.250%, 18.875%, and 21.500% (relative to 2019), tightening the required *CII* line beyond the earlier annual 2% trajectory [1].

Furthermore, the adoption of guidelines for measuring methane (CH_4) and nitrous oxide (N_2O) emissions and the establishment of a Well-to-Wake life-cycle assessment framework for fuels have been discussed, indicating that the regulatory scope is expanding beyond CO_2 alone toward a comprehensive GHG management regime [6].

Recent studies have examined the implications and compliance feasibility of the EEXI and *CII* regulations across diverse ship types. Scenario-based analyses demonstrated that the combined effects of design- and operation-based indices vary significantly depending on vessel category, highlighting the necessity of operational improvements alongside technical modifications [7].

Investigations focusing on tanker operations further revealed that propulsion optimization and engine retrofitting can improve both indices, although economic trade-offs may arise [8].

Other research proposed integrated monitoring frameworks that combine EEXI and *CII* evaluation, indicating that hybrid assessment methods enhance the reliability and fairness of performance monitoring [9].

In addition, modeling-based analyses showed that alternative fuel selection, voyage duration, and auxiliary load management have substantial effects on regulatory compliance, suggesting that proactive operational adaptation is essential to maintaining favorable *CII* ratings [10].

2.2. Efficiency Characteristics and Operating-Mode Studies of CPP

Previous work demonstrated that combination is superior at low load or speed and fixed at higher regimes, with a crossover near 0.525 load [11]. This study extends that finding to the *CII* context, quantifying the annual effect of mode selection.

A CPP adjusts blade pitch to match varying operating conditions, offering improved propulsive efficiency and maneuverability over fixed-pitch propellers. Geertsma, R.D.

has shown that pitch or speed co-ordination and adaptive pitch control can reduce fuel consumption and emissions while preventing engine overload, with reported savings in the 5–15% range under representative transit conditions [12]. A recent case analysis on Yangtze River vessels reports 5% fuel-consumption reduction from CPP operation optimization against conventional control, after calibrating the ship-performance model with experimental tests—consistent with the practical gains assumed in our scenarios [13].

Kim and Wang (2022) [14] comparatively analyzed a CPP-propelled vessel equipped with a medium-speed diesel engine under constant versus combined operating modes. Kim and Wang reported that near high-load (~3000 kW) the two modes exhibit broadly similar performance, whereas at medium and lower loads the combined mode delivers superior brake-specific fuel consumption and CO_2 emission rates. At a low-load point of 1250 kW, Kim and Wang found that the combined mode increased distance per unit fuel from 42–45 m/kg to ~70 m/kg, corresponding to an estimated 39.4% reduction in CO_2 per ton-mile. Kim and Wang concluded that for vessels with frequent low-speed operations—e.g., survey or research ships and trawlers—adopting the combined mode is effective for reducing fuel use and emissions [14].

Moon, Je, and Hwang (2024) experimentally investigated a two-stroke diesel with a controllable-pitch propeller under sailing conditions and showed that CPP mode selection materially affects both engine performance and exhaust emissions, with lower specific fuel consumption and reduced CO_2 when operated in the appropriate (combinator) regime [15].

Across multiple investigations, mode-specific speed–load curves intersect at a crossover where the relative efficiency of combinator and fixed modes reverses. Empirically, this occurs around mid-load (≈50%) for many single-screw CPP applications, implying a low-speed advantage for combinator and a medium- or high-speed advantage for the fixed mode. This crossover provides a principled basis for band-based mode selection in operations and is central to the present study's optimization scenarios [16].

Gao et al. (2023) [17] introduced the concept of an optimal combinator surface for CPP systems, proposing an efficiency-optimization methodology that maps propeller RPM and pitch set-points as a function of the required thrust. This demonstrates the feasibility of a system that can dynamically track the optimal operating point in real time in response to changing operating conditions [17].

2.3. Structural Issues in the CII Metric and Disadvantages for Short Voyages

The *CII* scheme calculated as annual CO_2 emissions divided by transport work has several noted limitations. According to a study by the International Chamber of Shipping (ICS), the current *CII* metric reflects trade patterns more strongly than a vessel's actual transport efficiency. In particular, because fuel consumption while the ship is not underway (e.g., port stays or berthing and cargo-handling operations) is included in the calculation, external factors outside the operator's control are disproportionately represented [18]. Braidotti et al. (2023) explicitly demonstrate that, for cruise ships, *CII* may be inconsistent with actual emissions trends due to large hotel loads and extended port times—motivating the functional correction we benchmark in this paper [3].

Recent Korean studies analyzed the applicability of EEXI and *CII* regulations to vessels exempt from IMO GHG control, focusing on training and government-operated ships. They found that ships with short voyages or long port-stay durations are structurally disadvantaged under current indices, suggesting that separate accounting of sailing and anchorage emissions is necessary for fair evaluation [19,20].

The reasons short-sea shipping vessels are structurally disadvantaged under the *CII* regime are threefold. First, short sailing distances increase the share of port-stay time, so CO_2 from generator and boiler operation raises the *CII* numerator without any increase in

distance, inflating the index. Second, if port-waiting time rises by 40%, the *CII* can increase by about 5 gCO_2/DWT-mile, potentially causing a two-grade downgrade, indicating that port-operations efficiency critically affects *CII*. Third, for special-purpose vessels such as training ships, operation of educational and training auxiliaries—although unrelated to transport work—is included in the *CII* calculation, introducing further distortion.

Proposed remedies in the literature include (i) extending accounting boundaries toward Well-to-Wake for fuel GHG intensities [21]; (ii) separating sea-passage from port operations in *CII* assessment (e.g., "pilot-to-pilot" concepts for sea-only benchmarking) [22]; and (iii) correction models that explicitly account for time at sea (*ts*) and hotel loads [3]. In this study, we operationalize a pragmatic hybrid denominator using an equivalent-distance construct for port-stay CO_2, and we benchmark it against a functional (Braidotti-type) correction fitted on monthly *ts*–*CII* data.

3. Methods

The methodology of this study consists of two main stages as follows:

(1) Data collection and baseline *CII* computation,
(2) *CII* correction and CPP simulation.

All experimental data processing, signal analysis, and visualization were performed using MATLAB R2025a (MathWorks, Natick, MA, USA; https://www.mathworks.com).

Figure 1 schematizes the procedural flow as the following order: data collection, baseline *CII* calculation, problem identification, application of correction models (Sea/Port hybrid and functional/Braidotti), CPP mode simulation, and results and recommendations.

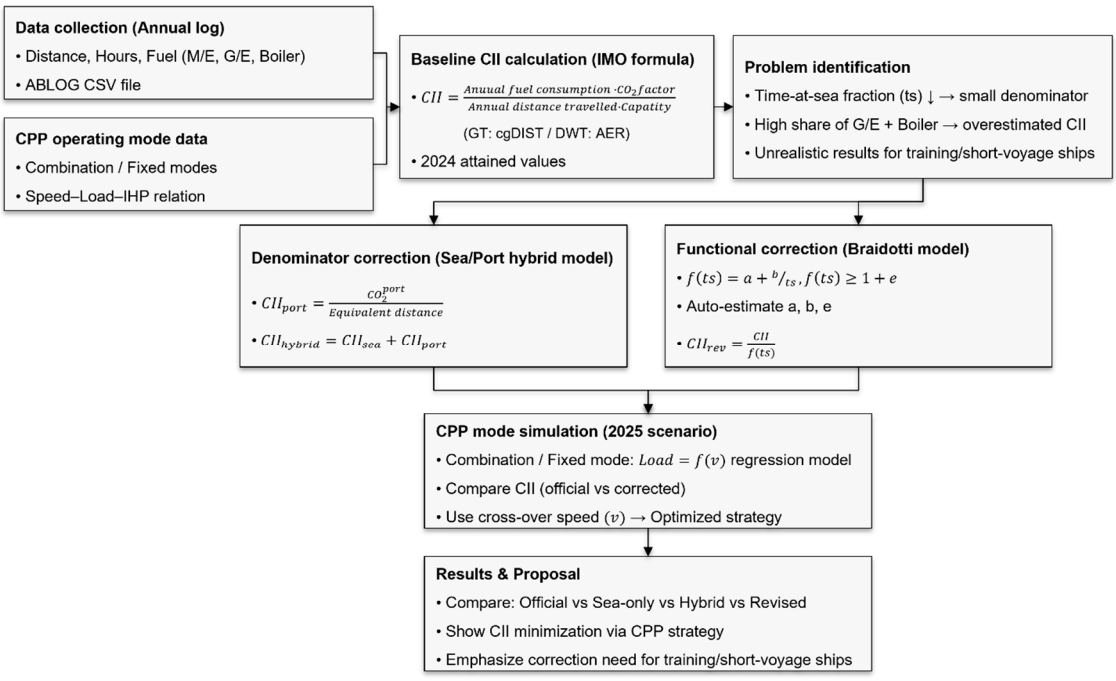


Figure 1. Methodological framework for *CII* correction and CPP mode optimization.

3.1. Data Collection and Baseline CII Computation

The principal particulars of the case-study vessel are summarized in Table 1. This study draws on two sources: the annual operating log (ABLOG) of the training ship and dedicated CPP operating data. Key variables include sailing distance, operating hours, and fuel consumption for the main engine, generators, and boiler, all consolidated in ABLOG files. In addition, we directly measured the mode-specific relationships among speed,

power, and indicated horsepower (IHP) for combinator and fixed CPP modes and merged these measurements into the dataset.

Table 1. Principal particulars of the case study vessel.

Item	Particular
Ship name	HANNARA
Ship type	Training/education
Gross tonnage	9196 GT
Deadweight tonnage	3671 DWT
Length overall (LOA)	113 m
Fuel	MGO
Main Engine	Hyundai-MAN B&W 6S40ME-B9.5-LP SCR
Speed (MCR)	146 rpm
Maximum continuous rating	6618 kW (MCR)
Propeller	Controllable Pitch Propeller

For CPP mode characterization, dedicated sea trials were conducted onboard the T/S Hannara. The CPP handle was gradually advanced from start-up in 5% load increments, and at each step the operating condition was held for approximately 30 s while recording engine and shaft parameters. Measurements were continued up to 95% CPP load, which corresponded to about 79% engine load in combination mode and 70% in fixed mode. Both CPP modes were tested in the same manner to ensure comparability. During the trials, the vessel carried 200 persons onboard, reflecting a full training complement. Although objective meteorological data were not recorded, the sea state was calm and did not impose notable disturbances on propulsion performance.

Figure 2 illustrates the measured torque–pitch characteristics of CPP under the two operating algorithms. In the combination mode, both propeller pitch and engine RPM are simultaneously controlled through the combinator governor, producing a smooth and progressive torque increase with speed. In contrast, the fixed mode maintains a constant engine RPM while varying only the propeller pitch, resulting in a steeper torque rise as the pitch increases. The color bar indicates the corresponding engine speed (RPM), clearly visualizing the control difference between the two CPP modes.

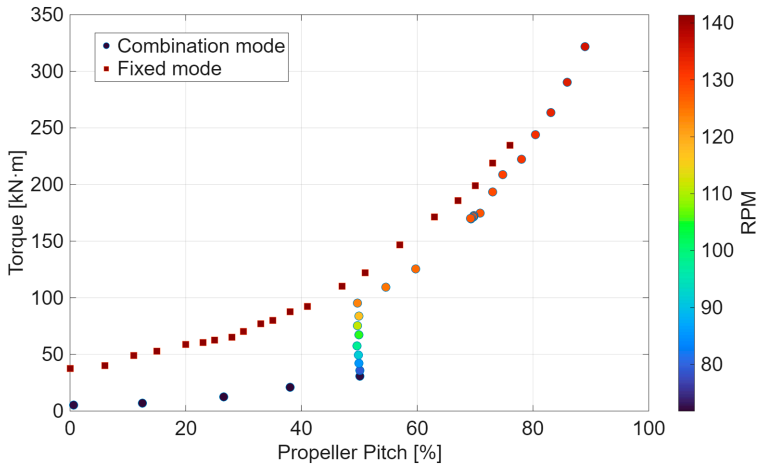


Figure 2. Comparison of torque–pitch characteristics under the two CPP control modes.

The training vessel, examined in this study, is not subject to MARPOL convention, and it is, in principle, outside the scope of mandatory *CII* calculation. Moreover, no dedicated *CII* formula or coefficients have been proposed for training vessels. Accordingly, considering that the ship carries no cargo and accommodates approximately 250 trainees, we adopt the official coefficients and derivation method proposed for the most analogous segment—cruise ships.

To determine the allowable *CII*, a vessel-specific reference value must first be established; this reference value is given by Equation (1) as the following:

$$CII_{ref} = a \cdot Capacity^{-c} \quad (1)$$

where a and c are coefficients derived from the 2019 IMO DCS data based on each vessel's capacity and its *CII* attainment value; for cruise passenger ships, a is 930 and c is 0.383. By applying the reduction rate Z to the vessel's reference value, the allowable *CII* is then calculated as shown in Equation (2):

$$required\ CII = (1 - \frac{Z}{100}) \times CII_{ref} \quad (2)$$

where Z is the year-by-year *CII* reduction factor relative to the 2019 reference value, and the reduction factors for 2023–2030 are shown in Table 2 [23].

Table 2. Year-by-year *CII* reduction factors (Z) relative to the 2019 reference (2023–2030).

Year	2023	2024	2025	2026	2027	2028	2029	2030
Z	5%	7%	9%	11%	13.625%	16.25%	18.875%	21.5%

The attained *CII* was calculated from annual fuel-consumption data, as shown in Equation (3):

$$attained\ CII = \frac{\sum(FC_j \times CF)}{Annual\ distance\ travelled \cdot Capatity} \quad (3)$$

where FC_j denotes the annual fuel consumption by fuel type j and CF is the fuel-specific conversion factor used to convert fuel consumption into CO_2 emissions. Capacity may be expressed as DWT or GT, and cruise ships use GT. Under IMO guidelines, annual emissions were obtained by multiplying fuel use by the fuel-specific CO_2 factor (CF; e.g., HFO = 3.114, MDO/MGO = 3.206, LNG = 2.750) [2], and the sailing distance was based on cgDIST. The analysis was conducted using the 2024 attained values.

The issues identified in this process are as follows:

- When the time-at-sea fraction (*ts*) is low, the denominator shrinks, and the *CII* is overestimated.
- A high share of generator (G/E) and boiler fuel consumption inflates the *CII*.
- For short-voyage operations and training vessels, the resulting *CII* can be unrealistic.

3.2. CII Corrections and CPP Simulation

To address these issues, we applied two correction approaches and then ran CPP-mode simulations.

3.2.1. Denominator Correction (Sea/Port Hybrid Model)

CO_2 emitted during port stays was converted into an equivalent distance (D_{equiv}) and added to the denominator of the official *CII*. The relationships are as the following:

$$V_{sea} = \frac{D_{sea}}{H_{sea}} \quad [\text{knots}] \tag{4}$$

$$D_{equiv} = V_{sea} \times H_{port} \quad [\text{nm}] \tag{5}$$

$$CII_{port} = \frac{CO_{2_port}}{D_{eqiuv} \times C_{GT}} \quad [\text{ton}/\text{gt}\cdot\text{nm}] \tag{6}$$

$$CII_{sea} = \frac{CO_{2_sea}}{D_{sea} \times C_{GT}} \quad [\text{ton}/\text{gt}\cdot\text{nm}] \tag{7}$$

where V_{sea} is annual average speed at sea [kn], D_{sea} is annual sailed distance [nm], H_{sea} is time at sea (sailing hours), CII_{port} is *CII* component based on port-stay CO_2, CII_{sea} is *CII* component based on at sea CO_2, CO_{2_sea} is at-sea CO_2 emission, CO_{2_port} is port-stay CO_2 emission, and C_{GT} is gross tonnage used as the capacity term in cgDIST as the following:

$$CII_{hybrid} = CII_{sea} + CII_{port} \quad [\text{ton}/\text{gt}\cdot\text{nm}]. \tag{8}$$

We explicitly separated at-sea emissions from port-stay emissions and thereby mitigated biases in the official *CII* for short-voyage, high port-stay operations.

3.2.2. Functional Correction (Braidotti Model)

We applied a time-at-sea–dependent correction to the official *CII* to counter inflation at low *ts*. The correction factor is as the following:

$$f(ts) = a + {}^{b}/_{ts}, f(ts) \geq 1 + e \tag{9}$$

where the coefficients *a*, *b*, and *e* were estimated to derive a curve that best approximates the relationship between the sailing time ratio (*ts*) and the empirically computed *CII*. Specifically, to account for the tendency of *CII* to be increasingly overestimated as *ts* decreases, the optimal coefficients *a*, *b*, and *e* were determined via a nonlinear least-squares regression fitted to the empirical data distribution. In this way, the function $f(ts)$ was designed to reproduce the distortion patterns observed in actual operational data. The revised *CII*, incorporating the final correction values, was then calculated as follows:

$$CII_{rev} = CII \times f(ts) \quad [\text{ton}/\text{gt}\cdot\text{nm}]. \tag{10}$$

Figure 3 illustrates the conceptual framework of the Braidotti functional correction. The correction term was defined as $dCII = d - b/t_s$, which sharply increased as the time-at-sea fraction t_s approached zero—representing months with little or no sailing and gradually decreased as t_s increased. The curve asymptotically converges to $CII = a$ at full-sea conditions ($t_s \to 1$), while the average cargo-ship condition was anchored at $t_s = 0.69$, where the correction became neutral. The upper and lower limits ($CII = c = a + d$ and $dCII = e = -15$) constrained over-correction at extremely low t_s values. This formulation captured the empirical pattern observed in monthly *CII* fluctuations—severe inflation during prolonged port stays and negligible bias during normal voyages—making it a suitable functional basis for the correction term, used in this study.

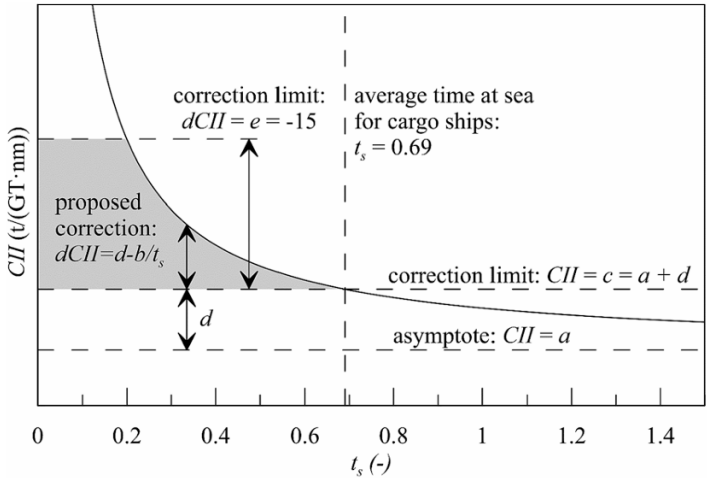


Figure 3. Conceptual illustration of the Braidotti functional correction [3].

In this study, we contrasted the functional correction proposed by Braidotti with a new denominator correction—the Sea/Port hybrid model—that we introduced. By comparing these two approaches, we evaluated their potential to alleviate the *CII* distortion that systematically affects short-voyage vessels.

Assuming a 2025 operating scenario, we modeled mode-specific speed–load relationships for CPP operation (combinator and fixed) using regression. On this basis, we compared the official *CII* with corrected *CII* values and, exploiting the crossover speed, propose an optimized operating strategy.

The objectives are threefold: (1) to compare official versus corrected *CII*—specifically sea-only, hybrid (denominator), and revised (functional/Braidotti); (2) to derive *CII*-minimizing strategies via CPP mode selection; and (3) to underscore the need for institutional denominator corrections to mitigate the structural disadvantage faced by short-voyage training vessels.

4. Results

This section presents the key findings from our data analysis and simulations. The results were organized into three parts: (1) a comparison between the official *CII* and corrected values, (2) an analysis of the speed–load relationships by CPP operating mode, and (3) the identification of the crossover point and its operational implications.

4.1. ABLOG-Based Annual Operating Data

Table 3 summarizes the 2024 monthly records from ABLOG for the main engine, generator engines, and boiler including fuel consumption, operating hours, and sailing distance.

The generator engines accumulated 4848 operating hours over the year—short of the 8760 h in a full year—because the vessel uses shore power during certain periods alongside port stays. By contrast, the boiler logged 8112 h (92.6% of the year), a markedly higher utilization than the generators. This is because the boiler was used not only for main engine warming but also for hotel services, space heating, and cooking for trainees and instructors on board. The main engine operated for 1548 h (17.7% of the year), reflecting the fact that, as seen in the ABLOG data, there were many months with no sailing. Operations of the training ship followed the academic calendar, with voyages concentrated during semester periods and little to no sailing outside those windows. These patterns reflected the short-voyage, education-and-training nature of the vessel.

Table 3. 2024 monthly ABLOG summary.

		Unit	Jan.	Feb.	Mar.	Apr.	May	Jun.	Jul.	Aug.	Sep.	Oct.	Nov.	Dec.	Total
Main Engine	Fuel	ton	0.0	0.0	55.5	55.5	117.5	5.5	0.0	26.2	31.6	43.7	168.9	0.0	504.3
	Time	hr	0	0	184	181	382	3	0	73	93	137	495	0	1548
	Distance	nm	0	0	2308	2341	4697	15	0	933	992	1697	7368	0	20,351
Generator Engine	Fuel	ton	0.2	7.0	22.4	18.9	62.9	118.3	121.3	125.8	106.1	40.5	104.5	0.3	728.3
	Time	hr	24	72	216	192	360	720	744	744	720	360	672	24	4848
Boiler	Fuel	ton	40.8	25.7	27.5	22.8	15.7	20.4	17.6	16.9	15.4	14.1	13.5	28.9	259.2
	Time	hr	744	672	744	648	648	720	744	600	672	672	504	744	8112

Generators account for more than half of total annual fuel consumption, attributable to their long operating hours and their role in supplying electrical power at sea and during port stays when shore power is unavailable. The main engine fuel use was concentrated in the sailing semesters and registered as zero in months without voyages. Taken together, these characteristics of operation and energy use help explain why the official *CII* can diverge from actual propulsive efficiency, and they constitute a primary source of bias in the metric for training ships.

4.2. Comparison Between Official and Corrected CII

Figure 4 plots monthly relationship between the attained *CII* and the time-at-sea fraction *ts* computed from ABLOG records (fuel consumption, sailed distance, and time at sea/at port). For each month, we show official *CII* from the IMO formula (blue circles), the hybrid *CII* obtained by adding port-stay CO_2 as an equivalent distance in the denominator (red triangles), and the Braidotti functional correction $f(ts)$ applied to the official value (gray squares). While at the annual level the time-weighted aggregation tends to dampen monthly fluctuations and bias, the monthly view makes clear how shorter sailing (smaller *ts*) is associated with greater dispersion and upward bias in the official *CII*. The hybrid correction visibly stabilizes low-*ts* months by reallocating port-stay emissions to the denominator, and the Braidotti curve tracks the empirical trend of inflation at small *ts* by construction.

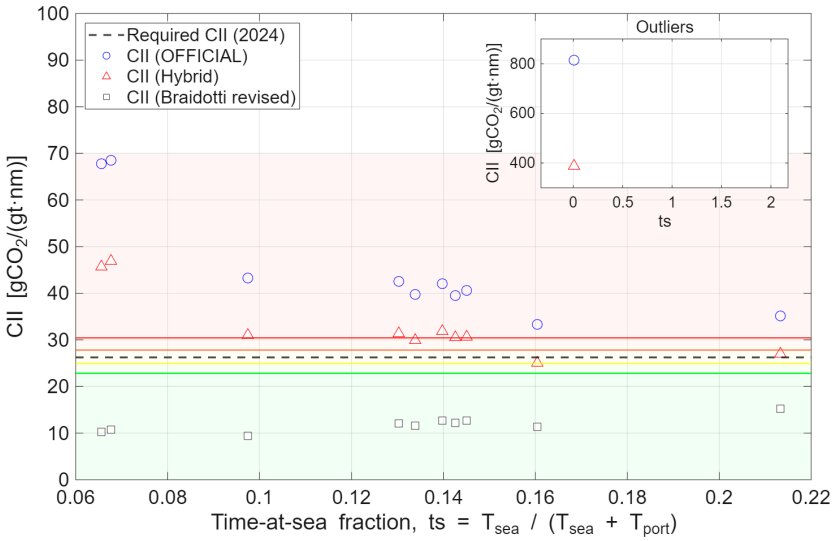


Figure 4. Monthly attained *CII* versus time-at-sea fraction.

The official *CII* rises sharply as the time-at-sea fraction *ts* decreases, producing unrealistically high values; in months with no or negligible sailing ($ts \approx 0$), the denominator collapses and outliers emerge (see inset). By contrast, the hybrid correction—by converting port-stay CO_2 to an equivalent distance—mitigates this denominator bias, yielding smoother and more stable *CII* values even at low *ts*. The Braidotti correction generally lowers the inflated official *CII*. However, when *ts* is extremely small, the factor $f(ts)$ becomes very large and over-correction occurs, leading in several low-*ts* months to *CII* values that fall unrealistically below the 2024 required line and associated rating thresholds.

In summary, for monthly or short-term assessments, the official formula alone is highly distorted, and the Braidotti approach carries a risk of over-correction at very low *ts*. The hybrid method provides more realistic and consistent results across the low-*ts* range. Thus, we recommend using hybrid as the default for short-voyage/short-cycle data, while applying Braidotti only above a data-driven threshold (e.g., $ts \geq ts_{min}$) and primarily for cruise-like operations.

4.3. Operating Profile: Speed–Time Distribution

Figure 5 aggregates the log by 0.5-kn speed bins and plots operating hours versus speed. The vertical dashed line marks 12 kn; speeds < 12 kn are shaded blue, and ≥12 kn orange. The distribution exhibits a clear two-regime structure around 12 kn. Most hours are concentrated in the 12–17 kn band, with a pronounced peak at 12–14 kn. By contrast, the dwell time in 10–12 kn is limited, and operations in 2–9 kn occur only intermittently, associated with berthing and unberthing and low-speed training activities.

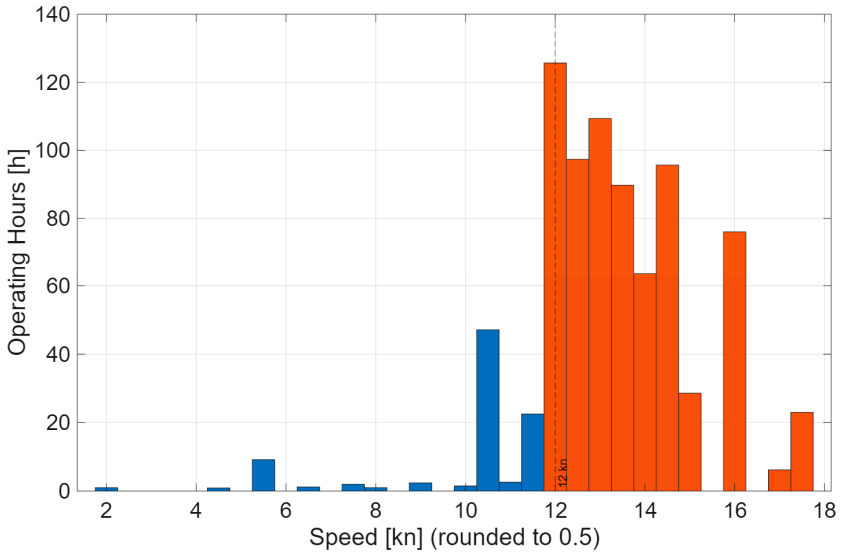


Figure 5. Annual operating hours by speed.

Figure 6 compare the speed–load relationships of the two CPP operating modes (combinator and fixed). To reduce noise, we first aggregated the raw scatter into bin means by speed (or load) intervals and then fitted cubic polynomials for each mode. The two curves in the figure intersect near 0.5 L and 12 kn. Below this point, the combination mode requires less load to achieve the same speed and is therefore advantageous. Additionally, the fixed mode becomes comparable or slightly superior. The high coefficients of determination (R^2 = 0.99) indicate that the mode-specific regressions explain the observations well. This crossover provides an operational basis for band-based mode selection: use combination in low-speed bands and fixed in medium- and high-speed bands.

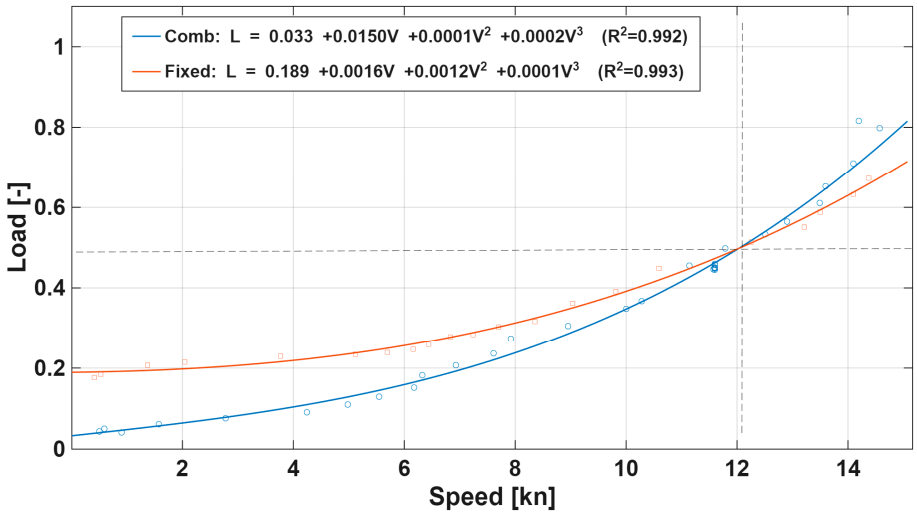


Figure 6. Load–speed regressions by CPP mode.

4.4. SFOC Curve and Fuel-Consumption Model

To quantitatively link ship speed to fuel consumption, we coupled the load-ratio SFOC curve with the main-engine specifications. The training ship was fitted with a HYUNDAI–MAN B&W 6S40ME-B9.5-LP SCR two-stroke engine (rated 6618 kW @ 146 rpm). Using the engine manual's reference value at 100% load, we set $SFOC_{baseline}$ = 173.4 g/kWh (Tier II, conventional turbocharger). The variation of *SFOC* with engine load was approximated following [24,25] as in Equation (11):

$$SFOC_{load} = SFOC_{baseline} \times \left(0.455 \times load^2 - 0.71 \times load + 1.28\right) \quad [\text{g/kWh}] \tag{11}$$

where load is the relative engine load, and $SFOC_{load}$ is the specific fuel-oil consumption at that load. Equation (11) reproduces the characteristic shallow U-shape, with a minimum in the NCR load is 0.7 to 0.9 range, consistent with typical two-stroke *SFOC* behavior. Figure 7 visualizes this curve and serves as the basis for computing speed-wise fuel flow and, subsequently, CO_2 per nautical mile as follows:

$$CO_{2,\text{per nm}}(v) = CF \times \frac{SFOC_{load}(L(v)) \cdot P(v)}{10^6 \cdot v} \quad [\text{ton}_{CO_2}/\text{nm}] \tag{12}$$

where, *CF* is fuel-specific CO_2 emission factor [tCO_2/t fuel], $SFOC_{load}$ is load-dependent specific fuel oil consumption [g/kWh], $L(v)$ is the speed–load function (dimensionless load ratio), $P(v)$ is an engine power [kW] ($P(v) = L(v) \times$ MCR), and v is ship speed [kn].

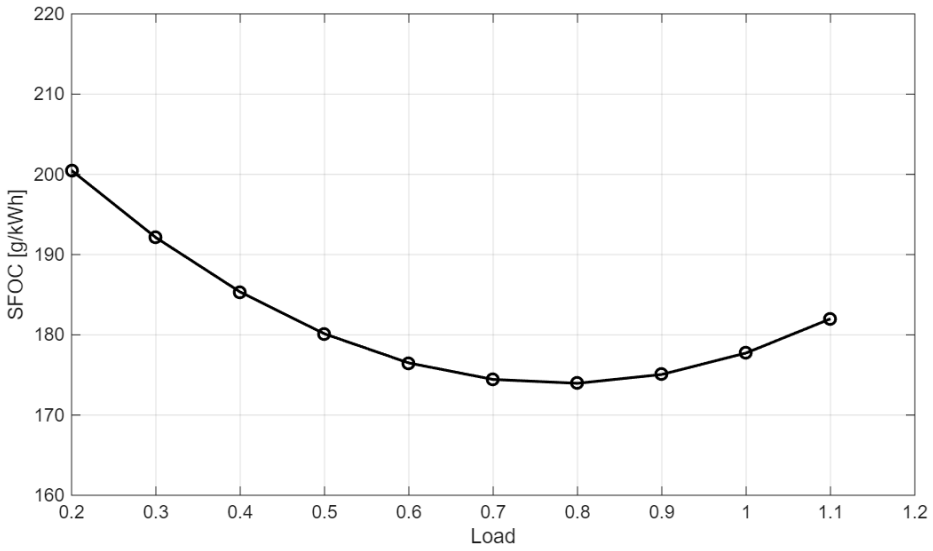


Figure 7. Specific fuel oil consumption (SFOC) versus engine load.

As shown in Figure 8, at low speeds, the combination mode achieves the same speed with lower required engine power and fuel use, yielding lower CO_2 per nautical mile. Near 12 kn the two curves touch (the crossover), and above ~12 kn the advantage shifts to fixed mode. The dashed bars on the right axis ("Operating hours") reflect the speed–time profile, showing that most operating time lies in the 12–16 kn band. In practice, this distribution supports a strategy of using fixed as the default for 12–16 kn passages, switching to combinator only in segments where low-speed dwelling is unavoidable due to route, weather, or training needs. The optimized schedule (combination at low speed, fixed at high speed) delivers a modest yet consistent improvement in annual *CII* relative to single-mode operation across the whole range.

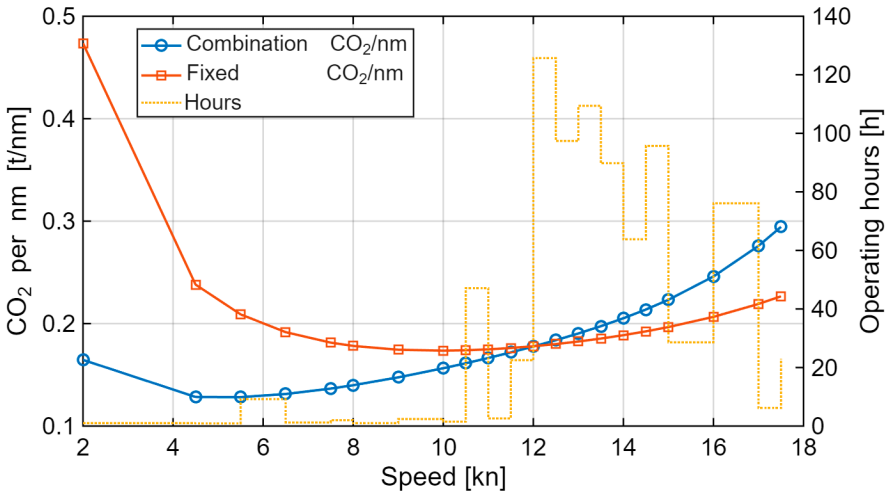


Figure 8. CO_2 per nautical mile versus speed by CPP mode (combinator versus fixed).

4.5. Corrected CII Comparison (2024 Attained Versus 2025 Scenarios)

Table 4 summarizes the meaning and basis of each symbol used in Figures 9 and 10. This table clarifies how each correction method (official, sea-only, Braidotti adjustment, equivalent distance, and hybrid) and the modeled 2025 scenarios are represented in the plots.

Table 4. Description of symbols used in Figures 9 and 10.

Symbol	Label	Description/Basis
-----	Requried *CII*	IMO regulation curve for cruise passenger ships (GT-based denominator)
●	Attained 2024 (official)	Official 2024 *CII* (cgDIST, GT basis). Includes all fuel (M/E, G/E, Boiler) divided by GT·nm
△	Attained 2024 (sea-only)	2024 *CII* computed using only sailing periods excluding port-stay hours and fuel
◇	Attained 2024 (Braidotti-adj)	2024 *CII* corrected by Braidotti method, which applies a time-at-sea fraction function $f(ts)$ to mitigate denominator shrinkage
✱	Attained 2024 (equiv-dist)	2024 *CII* adjusted by equivalent-distance method: port hours converted into distance using average sailing speed
▲	Attained 2024 (hybrid)	2024 *CII* by hybrid denominator: ME emissions normalized by sailing distance, hotel (GE/boiler) emissions normalized by time × average speed
○	Modeled 2025 (combination)	2025 *CII* projected *CII* using regression-based load–speed curve for CPP combination mode, matched with 2024 operating profile
□	Modeled 2025 (fixed)	Same as above, but for CPP fixed mode
☆	Modeled 2025 (optimized)	Modeled 2025 *CII* under optimized schedule (combination at low speeds, fixed at higher speeds)
•	Modeled 2025 (comb, hybrid)	Combination mode with hybrid denominator correction
■	Modeled 2025 (fixed, hybrid)	Fixed mode with hybrid denominator correction
★	Modeled 2025 (opt, hybrid)	Optimized combination/fixed switching with hybrid denominator correction

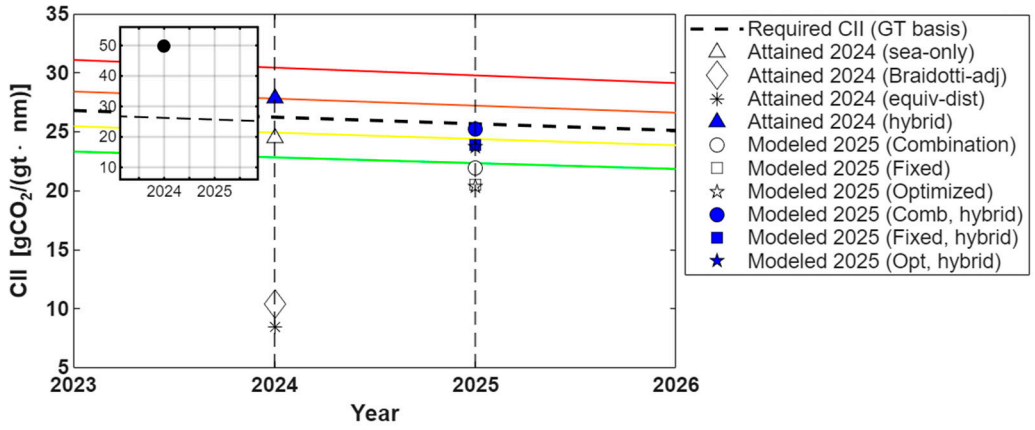


Figure 9. *CII* comparison—2024 attained versus 2025 modeled. The colored lines indicate rating thresholds (A–E); detailed separation is provided in Figure 10.

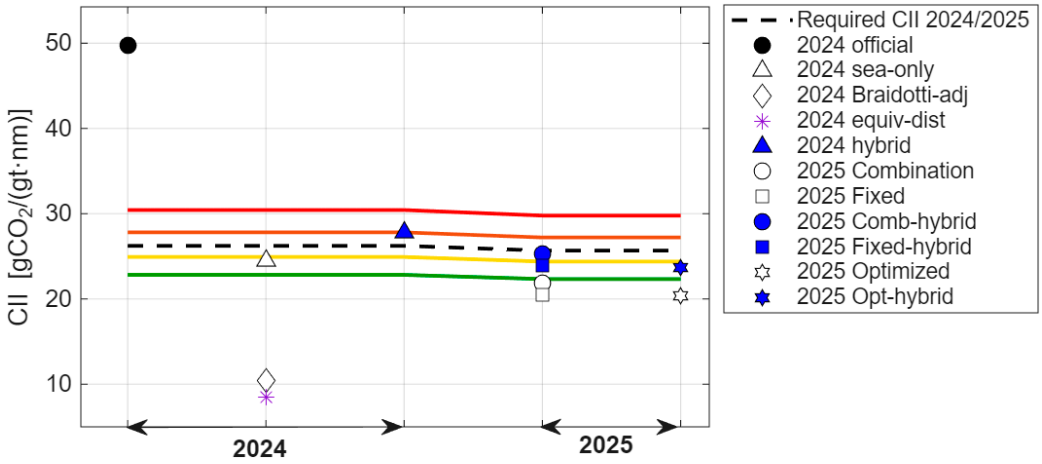


Figure 10. Stepwise *CII* adjustments—2024 (official → sea-only → Braidotti → equivalent distance → hybrid) and 2025 CPP scenarios (combination, fixed, optimized; with and without hybrid), expanded from Figure 9 for clarity.

Figure 9 compares the 2024 attained values with the 2025 scenario results to summarize how the choice of correction method and CPP operating mode affects *CII*. Figure 10 unpacks the same results step-by-step, clarifying the contribution of each adjustment. We start from the official 2024 *CII* (cgDIST, GT basis), which is inflated relative to the required line because of short voyages and substantial port-stay shares. Applying the sea-only variant (counting at-sea fuel only) partly reduces this bias. Adding the Braidotti functional correction yields a further overall decrease; however, when the time-at-sea fraction *ts* is very small, the correction factor $f(ts)$ grows large and can over-correct, producing values unrealistically below the 2024 required line and rating thresholds. In contrast, the equivalent-distance denominator adjustment coheres with the operating reality of long port stays; combined with sea-only (hybrid), it shrinks monthly dispersion and brings the annual value back toward a realistic vicinity of the required line.

For 2025, we recomputed main-engine fuel using the 2024 speed–time profile and three CPP strategies: all-combinator, all-fixed, and a speed-band optimized schedule that selects the mode with the lower CO_2/nm at each speed. The results are as follows: First, considering the engine alone, all-fixed is consistently lower in *CII* than all-combinator over the year. Second, the optimized schedule (combinator at low speeds < ~12 kn, fixed at ≥~12 kn) provides a modest but consistent additional reduction relative to all-fixed. Third, when the equivalent-distance denominator is added (comb-hybrid, fixed-hybrid,

opt-hybrid), the values shift downward in a conservative and consistent way; notably, opt-hybrid falls below the required line and meets the B-rating criterion.

Overall, the 2024 stepwise analysis shows that the hybrid approach is the most reasonable remedy for the structural bias of the official formula under short-voyage, high-port-stay conditions. The 2025 simulations demonstrate that crossover-based mode selection yields tangible, if incremental, *CII* gains. While the Braidotti correction can be effective for longer-*ts* or cruise-like operations, it risks over-correction when *ts* is very small; hence, for practical application to short-voyage training ships, we recommend adopting hybrid as the default and using Braidotti only above a data-driven *ts* threshold.

5. Discussion

This study quantitatively diagnosed the structural limitations of the official *CII* formula for a training ship with short-voyage, short-cycle operations, and proposed a practical response that combines a denominator (hybrid) correction with a CPP mode strategy. In operating patterns with a large share of port stays, separating at-sea and in-port emissions and allocating the latter to an equivalent distance proved effective in alleviating overestimation; moreover, mode selection by speed band further reduced carbon intensity.

In short-voyage or port-intensive operations, the official *CII* tends to be systematically high because port-stay fuel is divided by the same transport-work denominator. Converting port-stay emissions to equivalent distance (D_{equiv}) and using the hybrid denominator reduced month-to-month dispersion and brought the annual value back toward the required line. The CPP mode selection also mattered and combining the measured speed–load regressions with the *SFOC* model showed that combination is advantageous at low speeds, while fixed becomes preferable at medium and high speeds. An optimized schedule that switches modes by speed band delivered a modest additional improvement over all-fixed operation. However, when *ts* is extremely small, the Braidotti functional correction can be overcorrect; it is therefore best used as a supplement above a threshold value of *ts*.

Additionally, the boiler onboard operates almost continuously (≈8112 h annually), contributing substantial emissions during port stays. Under the official *CII* formula, these are divided by a very small sailing distance denominator, artificially inflating the attained *CII*. The hybrid denominator corrects for this distortion by separating at-sea and in-port emissions and converting port-related boiler fuel use into an equivalent distance, thereby capturing the actual operational profile of training ships more accurately.

The 2024 fuel use in this study was estimated by combining the SFOC curve with speed–load regressions; it may deviate from fuel measured by flowmeters or bunker records. Engine condition (hull fouling, maintenance, intake/exhaust), environmental forces (waves, wind, currents), variability in auxiliary loads, and assumptions on fuel properties and *CF* can introduce error in *SFOC* and load estimates. Consequently, the *CII* values and ratings shown in the figures should not be interpreted as exact absolutes; applying actual fuel data may yield higher *CII*. Monthly *CII* for months with little or no sailing is particularly sensitive to denominator shrinkage, so annual or semester-level aggregation is recommended for conservative interpretation.

To further examine the robustness of the CPP mode crossover, we incorporated fuel-specific baseline *SFOC* values (164.1 g/kWh for MGO, 175.0 g/kWh for HFO, and 141.0 g/kWh for LNG) together with the corresponding IMO CO_2 conversion factors (3.206, 3.114, and 2.750 tCO_2/t fuel). The results (Appendix A Figure A1) show that while absolute CO_2 per nm values shift depending on fuel type—highest for MGO, intermediate for HFO, and lowest for LNG—the crossover speed (~12 kn) and the relative superiority of combination at low speeds versus fixed at higher speeds remain unchanged. This confirms that the proposed operational strategy is valid irrespective of the specific fuel employed.

For ship types and business models with long port-stay shares, a sea/port split in the metric (e.g., the hybrid or equivalent-distance approach) is needed. On the operations side, it is reasonable to define vessel-specific crossover rules around ~12 kn based on regression fits, planning fixed as the default for route passages and combination for low-speed dwelling segments driven by weather, traffic, or training. To raise the reliability of *CII* reporting, operators should adopt voyage-level analytics that integrate fuel flowmeters, shaft-power meters, AIS, and weather data.

We will cross-validate against actual fuel measurements to quantify bias in *SFOC*-based estimates, and bound the effect of variations in *SFOC* baseline, *L-v* coefficients, and *CF* by sensitivity analysis. The framework can be extended to online optimization that recommends real-time mode switching using sea-state/traffic forecasts. Finally, to avoid reliance on cruise-segment surrogates, we aim to propose training ship-specific factors and corrections, thereby improving generalizability and credibility.

This study is based on data from a single training vessel; therefore, the quantitative results should not be generalized directly to all ship types. The methodological framework, however, is generic and can be replicated for other ships once their operational logs are available. Future work will extend the analysis to multiple training and short voyage vessels to confirm consistency across hull forms and service profiles.

6. Conclusions

Within the IMO decarbonization context, this case study on a short-voyage training ship quantitatively examined structural biases in *CII* calculation and presented a practical framework that combines a hybrid (denominator) correction with the CPP mode scheduling. Our goals were to (1) characterize the size and shape of the time-at-sea (*ts*) bias in monthly data, (2) compare the efficacy and limits of hybrid versus Braidotti corrections, and (3) quantify the *CII* impact of a crossover-based CPP strategy.

The analysis confirmed that in monthly or short-term assessments, the official *CII* rises sharply as *ts* decreases and can produce outliers when sailing is minimal. The hybrid correction stabilized values even at low *ts*. The Braidotti correction reduced overestimation on average but posed an over-correction risk when *ts* is approximately zero, suggesting its use as a supplement above a threshold. The CPP mode analysis revealed a crossover near 12 kn (≈50% load): combination at low speed and fixed at medium and high speed. Under 2025 scenarios using the 2024 operating profile, all-fixed outperformed all-combinator, while optimized (combination at low, fixed at high speeds) yielded a further, modest reduction. Notably, opt-hybrid (optimized + hybrid denominator) fell below the required line and met the B-rating.

These results imply that for training ships—with high port-stay shares and academic-calendar operations—sea/port separation and speed-band mode selection are key levers for *CII* management. Despite the absence of a MARPOL *CII* and of training-ship-specific factors, the framework provides a coherent basis for decision-making by leveraging cruise-segment required lines only for comparability.

Finally, because 2024 fuel use was *SFOC*-based, the reported *CII* and ratings should be interpreted conservatively and may be higher with actual fuel data. Future work should include cross-checks with measured fuel, sensitivity studies on SFOC, *L-v* coefficients, and *CF*, real-time optimization with sea-state inputs, and training-ship-specific adjustment factors. In summary, the integrated hybrid plus CPP framework offers a practical roadmap for reducing bias and achieving rating compliance for short-voyage vessels, with low data requirements and high potential for extension to other ship types and operating models.

Author Contributions: Conceptualization, J.-W.L.; methodology, J.-W.L. and Q.D.V.; software, Q.D.V. and J.-W.L.; validation, J.-W.L., Q.D.V. and J.-U.L.; formal analysis, J.-W.L. and Q.D.V.; investigation,

J.-W.L.; resources, J.-U.L.; data curation, J.-W.L. and Q.D.V.; writing—original draft preparation, J.-W.L.; writing—review and editing, J.-U.L., Q.D.V. and J.-W.L.; visualization, J.-W.L. and Q.D.V.; supervision, J.-U.L.; project administration, J.-U.L.; funding acquisition, J.-U.L. All authors have read and agreed to the published version of the manuscript.

Funding: This research was supported by two projects funded by the Ministry of Oceans and Fisheries (MOF, Korea) through the Korea Institute of Marine Science & Technology Promotion (KIMST): Development of Autonomous Ship Technology (Project No. 20200615), Development of integrated management system for GHG emissions from ships (Project No. RS-2023-00256331).

Institutional Review Board Statement: Not applicable.

Informed Consent Statement: Not applicable.

Data Availability Statement: The original contributions presented in this study are included in the article. Further inquiries can be directed to the corresponding author.

Acknowledgments: During the preparation of this manuscript, the authors used ChatGPT(GPT-5, OpenAI, San Francisco, CA, USA; https://chat.openai.com) to improve clarity and readability of the text. The authors have reviewed and edited all generated content and take full responsibility for the final version of the manuscript.

Conflicts of Interest: The authors declare no conflict of interest.

Abbreviations

a, c	Regression coefficients for reference *CII*, derived from 2019 IMO DCS data
AER	Annual Efficiency Ratio (CO_2 per DWT·nm)
ALB	Available lower berths (used for cbDIST in cruise segment)
CII	Carbon Intensity Indicator
CF	Fuel-specific CO_2 conversion factor
cbDIST	Capacity ALB (the number of available lower berths) distance
cgDIST	Capacity gross ton distance
D	Annual sailed distance
D_{equiv}	Equivalent distance converted from port hours
EEXI	Energy Efficiency Existing Ship Index
GT	Gross tonnage
IHP	Indicated horsepower
L	Engine load ratio
MCR	Maximum continuous rating
ME	Main engine
GE	Generator engine
BLR	Boiler
$P_m(v)$	Engine power at speed v in CPP mode m
SFOC	Specific fuel-oil consumption
$SFOC_0$	Baseline SFOC at 100% load
ts	Time-at-sea fraction
T_{sea}, T_{port}	Sailing hours, port-stay hours
V	Ship speed
Z	*CII* annual reduction factor relative to 2019 reference
α	Weighting factor for equivalent-distance contribution
$f(ts)$	Functional correction factor (Braidotti model)

Appendix A

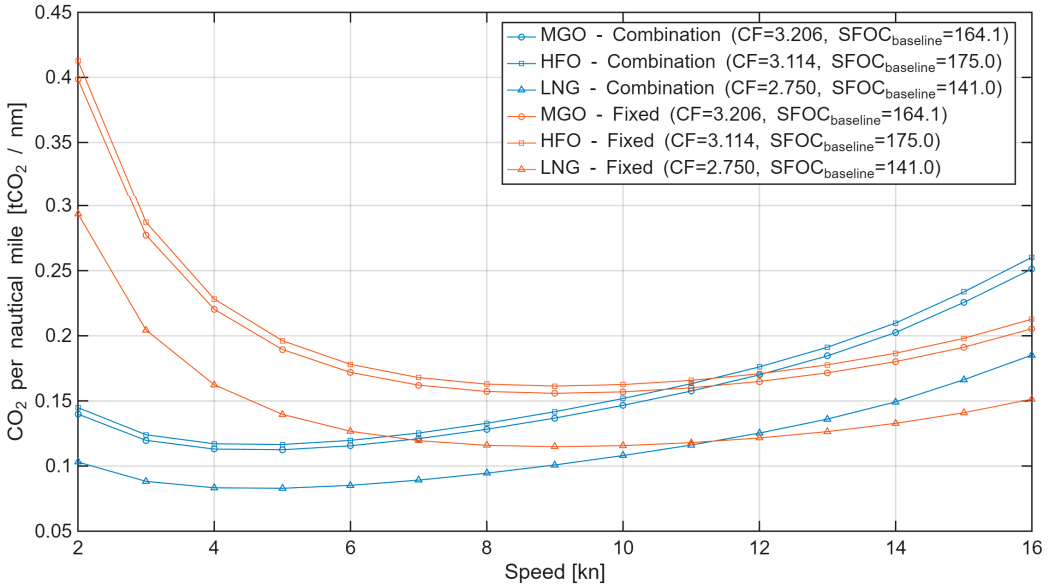


Figure A1. Fuel-specific CO_2 emissions per nautical mile as a function of ship speed under combination and fixed CPP modes. The baseline SFOC values were set to 164.1 g/kWh for MGO, 175.0 g/kWh for HFO, and 141.0 g/kWh for LNG, with corresponding IMO CO_2 emission factors of 3.206, 3.114, and 2.750 tCO_2/t fuel, respectively. Although the absolute emission levels vary by fuel type, the relative advantage of combination at low speeds and fixed at higher speeds remains consistent, with the crossover point near ~12 kn.

References

1. IMO. *Report of the Marine Environment Protection Committee on Its Eighty-Third Session (MEPC 83/24)*; International Maritime Organization (IMO): London, UK, 2025.
2. IMO. *2018 Guidelines on the Method of Calculation of the Attained Energy Efficiency Design Index (EEDI) for New Ships*; International Maritime Organization (IMO): London, UK, 2018.
3. Braidotti, L.; Bertagna, S.; Rappoccio, R.; Utzeri, S.; Bucci, V.; Marinò, A. On the Inconsistency and Revision of Carbon Intensity Indicator for Cruise Ships. *Transp. Res. Part Transp. Environ.* **2023**, *118*, 103662. [CrossRef]
4. International Maritime Organization. EEXI and CII—Ship Carbon Intensity and Rating System. Available online: https://www.imo.org/en/mediacentre/hottopics/pages/eexi-CII-faq.aspx (accessed on 5 September 2025).
5. International Maritime Organization. Improving the Energy Efficiency of Ships. Available online: https://www.imo.org/en/ourwork/environment/pages/improving%20the%20energy%20efficiency%20of%20ships.aspx (accessed on 5 September 2025).
6. Class, N.K. *Preliminary Report of IMO MEPC 83*; Nippon Kaiji Kyokai: Chiyoda City, Japan, 2025.
7. Bayraktar, M.; Yuksel, O. A Scenario-Based Assessment of the Energy Efficiency Existing Ship Index (EEXI) and Carbon Intensity Indicator (*CII*) Regulations. *Ocean Eng.* **2023**, *278*, 114295. [CrossRef]
8. Vasilev, M.; Kalajdžić, M.; Momčilović, N. On Energy Efficiency of Tankers: EEDI, EEXI and *CII*. *Ocean Eng.* **2025**, *317*, 120028. [CrossRef]
9. Kim, H.; Yeo, S.; Lee, J.; Lee, W.-J. Proposal and Analysis for Effective Implementation of New Measures to Reduce the Operational Carbon Intensity of Ships. *Ocean Eng.* **2023**, *280*, 114827. [CrossRef]
10. Bayramoğlu, K. The Effects of Alternative Fuels, Cruising Duration and Variable Generators Combination on Exhaust Emissions, Energy Efficiency Existing Ship Index (EEXI) and Carbon Intensity Rating (*CII*). *Ocean Eng.* **2024**, *302*, 117723. [CrossRef]
11. Lee, J.-W.; Vuong, Q.D.; Jeong, E.-S.; Noh, J.-H.; Lee, J.-U. Efficiency Comparison and Optimal Voyage Strategy of CPP Combination and Fixed Modes Based on Ship Operational Data. *Appl. Sci.* **2025**, *15*, 10435. [CrossRef]
12. Geertsma, R.; Visser, K.; Negenborn, R. Adaptive Pitch Control for Ships with Diesel Mechanical and Hybrid Propulsion. *Appl. Energy* **2018**, *228*, 2490–2509. [CrossRef]
13. Tian, W.; Lang, X.; Zhang, C.; Yan, S.; Li, B.; Zang, S. Optimization of Controllable-Pitch Propeller Operations for Yangtze River Sailing Ships. *J. Mar. Sci. Eng.* **2024**, *12*, 1579. [CrossRef]
14. Kim, S.-A.; Wang, W.-G. A Study of Engine Performance and Exhaust Emission Characteristics of CPP Propulsion Ship with Operating Mode. *J. Power Syst. Eng.* **2022**, *26*, 91–100. [CrossRef]

15. Moon, J.-S.; Je, M.-A.; Hwang, S.-C. A Study on Performance and Exhaust Emission Characteristics According to the Controllable Pitch Propeller Operation of Two-Stroke Diesel Engine in Sailing Condition. *J. Adv. Mar. Eng. Technol.* **2024**, *48*, 384–391. [CrossRef]
16. Borba, M. Understanding Load Calculation in Thrusters: Fixed Pitch (FPT) and Controllable Pitch Propellers (CPP)—Part 2. LinkedIn 2025. Available online: https://www.linkedin.com/pulse/understanding-load-calculation-thrusters-fixed-pitch-fpt-borba-4tzbf (accessed on 4 September 2025).
17. Gao, F.; Bloch, F.; Brodtkorb, A.H. Novel Combinator Surface Concept for Efficiency Optimization of Ship Propulsion System. *Ocean Eng.* **2023**, *280*, 114489. [CrossRef]
18. International Chamber of Shipping. *Energy Efficiency of Ships—Key Drivers of the CII Rating System*; International Maritime Organization (IMO): London, UK, 2025.
19. Lim, H.-G.; Han, K.-Y.; Lee, J.-W. A Study on the Application of EEXI to Ships Exempted from GHG Reduction Measures. *J. Korean Soc. Mar. Environ. Energy* **2023**, *26*, 349–358. (In Korean) [CrossRef]
20. Han, K.-Y.; Lim, H.-G.; Lee, J.-W. A Study on the Application of *CII* Regulations for Ships Exempt from GHG Regulations. *J. Korean Soc. Mar. Environ. Energy* **2025**, *28*, 108–116. (In Korean) [CrossRef]
21. Nelissen, D.; Kleijn, A.; Hilster, D. *CII and EU Maritime Decarbonisation*; CE Delft: Delft, The Netherlands, 2023.
22. Stolt-Nielsen Limited. *The Carbon Battle: Is CII out of Scope with the Real World?* Stolt-Nielsen Limited: London, UK, 2024.
23. Kim, H. *IMO News Flash MEPC 83*; Conv. Legis. Serv. Team; Korean Register (KR): Busan, Republic of Korea, 2025. Available online: https://www.krs.co.kr/TECHNICAL_FILE/IMO%20News%20Flash(K)%20MEPC%2083.pdf (accessed on 4 September 2025).
24. Lee, J.-U.; Lee, W.-J.; Jeong, E.-S.; Noh, J.-H.; Kim, J.-S.; Lee, J.-W. Algorithm for Monitoring Emissions Based on Actual Speed of Ships Participating in the Korean Vessel Speed Reduction Program. *Energies* **2022**, *15*, 9555. [CrossRef]
25. International Maritime Organization. *Fourth IMO Greenhouse Gas Study (2020)*; International Maritime Organization: London, UK, 2020.

Disclaimer/Publisher's Note: The statements, opinions and data contained in all publications are solely those of the individual author(s) and contributor(s) and not of MDPI and/or the editor(s). MDPI and/or the editor(s) disclaim responsibility for any injury to people or property resulting from any ideas, methods, instructions or products referred to in the content.